



Association of DEXA with EDX in Evaluation of Inorganic Bone Components After Application of Nano bone For Repair of Bone Defect

Naglaa Elkilania¹, Nehad A. Ahmad^{2*}

Codex : 05/2022/10

Aadj@azhar.edu.eg

KEYWORDS

Nano bone, DEXA, EDX,
Rabbits, bone mineral

ABSTRACT

Aim: The aim of this study is to correlate DEXA and EDX in assessment the variations in chemical composition in terms of the main elements comprising the bone mineral {calcium (Ca), and phosphorus (P)} after application of Nano bone for Repair of bone defect. **Subjects and Methods:** A bone drill defect was created in the right tibia (two holes in each tibia) of 48 rabbits; upper hole was left empty while the lower hole was packed with NanoBone. 24 animals were sacrificed 2 weeks after surgery; the remaining animals were sacrificed after 4 weeks. Half of the bone specimens prepared for the routine laboratory processing, histological and histomorphometric, while The remaining specimens were scanned by Dual-energy X-ray absorptiometry (DEXA) for bone mineral density measurement and then used for bone mineral composition determination by Energy Dispersive X-ray Analyses (EDX). The measurements of DEXA and EDX have been compared after that, data were submitted to ANOVA and Tukey's test. **Results:** DEXA showed a strong positive correlation with EDX and histological analysis. **Conclusion:** Energy-dispersive X-ray microanalysis (EDX) is a useful quantitative tool for the analysis of Ca and P in bone in a non-invasive way.

INTRODUCTION

Bone is a specialized connective tissue undergo remodeling and rebuilding throughout an individual life. It is a scaffold of the body which is responsible for support, locomotion, protection and load bearing. In addition, it is responsible for hematopoiesis, mineral homeostasis ⁽¹⁾.

The unmineralized phase or osteoid consists mainly of organic component which accounts for approximately 25% of the weight of bone matrix. It includes type I collagen (~90%) and other non-collagenous proteins (for example, sialoprotein and osteopontin). The non-collagenous proteins and proteoglycans account for a small total weight of organic component, though they still have an important role in osteoblast differentiation and tissue mineralization ⁽²⁾. The mineralized phase of the bone is composed of hydroxyl-apatite [Ca₁₀(PO₄)₆(OH)₂] in

1. Department of Oral Medicine, Periodontology, Oral Diagnosis and Dental Radiology, Faculty of Dental Medicine, Al-Azhar University, Cairo (girls), Egypt.
2. Department of Oral and Dental Biology, Faculty of Dental Medicine, Al-Azhar University, Cairo (girls), Egypt.

* Corresponding Author e-mail:
nehadmuhammed.26@azhar.edu.eg

a crystalline form. Structurally specific for bone. However, with a variable crystallinity depending on the stage in the mineralization process and age⁽³⁾. In addition, a number of other elements are incorporated in bone in trace amounts and a constant remodeling activity including an ion exchange with other compartments. Ca and P are the main elements of the mineral matrix and their concentrations vary independently. Ca is the most abundant cation in the body (approximately 99%) is present in the mineral phase. The remaining 1% is present within the extracellular and intracellular fluids. Likewise, body phosphate (approximately 85%) is present in the mineral phase of bone. Ca and phosphate interact in many fundamental processes in the body due to hormonal and physicochemical factors⁽⁴⁾. The relative content of Ca and P, however, is critical for sustaining mineral homeostasis and bone metabolism and their co-dependence is evident for bone growth and development⁽⁵⁾. It is therefore a suitable biomarker for the assessment of bone health⁽⁶⁾.

The Energy-dispersive x-ray (EDX) analytical method provides a useful tool for simultaneous elemental quantification in bone. It has the advantage of permitting the use of regular bone biopsy material and thus allowing for a unique microstructural evaluation of the degree of mineralization. By comparison with other established methods, the EDX microanalysis involves analysis of x-rays with energies characteristic of the atoms in the specimen emitted when an incident electron hits the specimen surface⁽⁷⁾. Analysis of these x-rays can provide elemental maps of the distribution of important elements such as Ca, P, F, and Sr within the specimen⁽⁸⁻¹¹⁾.

Current clinical methods utilize dual X-ray absorptiometry (DXA) as the gold standard for in vivo noninvasive measurements for areal BMD. It uses less than 1/10th the dose of a standard chest x-ray⁽¹²⁾. The DEXA scan is typically used to diagnose osteoporosis and assess an individual's risk for developing fractures.⁽¹³⁾ Many studies reported that the dual energy X-ray absorptiometry (DXA) proved successful to monitor BMD changes after incorporation of different types of bone grafts⁽¹⁴⁾.

Even though bone tissue has internal repair and regeneration capacity, healing of large-scale bone defects caused by trauma, infection and tumor still needs external interventions⁽¹⁾. Therefore, a huge demand for technologies and materials to ameliorate such kind of maladies. A group of these synthetic biomaterials are termed osteoinductive biomaterials. In vivo environment these bone graft substitutes are able to form bone, This refers to their ability to stimulate and support the proliferation and differentiation of mesenchymal progenitor cells of the host tissue when implanted in ectopic sites, together with the induction of bone formation⁽¹⁵⁻¹⁸⁾.

NanoBone graft material (one of these osteoinductive biomaterials) is a recently developed and approved granular material used in bone regeneration; it consists of synthetic nanocrystalline hydroxy-apatite embedded in a silica gel matrix mimicking the structure of normal bone tissue⁽¹⁹⁾. NanoBone graft possesses several properties that enhance bone regeneration. It has similar architecture to normal bone which enhances blood circulation within the NanoBone graft⁽²⁰⁾. The nano-roughness on the surface of the graft is the same as that of normal bone which provides a better medium for osteoblasts to grow and function⁽²¹⁾. It also has a large surface area to volume ratio that increases adsorption of proteins such as fibronectin and vitronectin which mediate osteoblastic adhesion. So unlike other synthetic bone substitutes, NanoBone graft has osseointegrative and osseopromotive properties^(22,23). The special structure of NanoBone results in an extremely fast bone formation. NanoBone may also be dosed with antibiotics which are released when bacteria enter the site of the joint replacement improving the chances of the implant being accepted by the body⁽²⁴⁾. Animal experiments using this nanocrystalline hydroxy-apatite (nCHA) in the mini pig critical size defect model showed a significantly higher rate of bone formation compared to other HA and tricalcium phosphate (TCP) materials or gelatin sponges and a nearly complete resorption 8 months after implantation⁽²⁵⁾.



MATERIALS AND METHODS

This study were held according to the recommendations of the ethics committee in the animals' experimentation of the faculty (REC-PD-21-05)

The sample size calculation

We used Steven K. Thompson equation to calculate the sample size, from the next formula:

$$n = \frac{Nxp(1-p)}{\{(N-1)(d \div Z^2)\} + p(1-p)}$$

Where:

n: sample size (42.77)

N: Population size (48)

Z: Confidence level at 95% (1.96)

d: Error proportion (0.05)

p: Probability (50%)

Surgical procedures

A bone drill defect (3mm) was created in the right tibia (two holes in each tibia) of 48 rabbits, upper hole was left empty while the lower hole was packed with NanoBone. 2 weeks after the surgery, 24 rabbits were sacrificed. The remaining animals were sacrificed 4 weeks after the surgery that created the bone defect. After the sacrifice, the tibiae were removed, Half of the The bone specimens (12 tabiae) prepared for the routine laboratory processing, histological and histomorphometric, while The remaining specimens (12 tabiae) for bone mineral composition determination by electron microprobe analysis (EDX) and for bone mineral density by Dual-energy X-ray absorptiometry (DEXA) machine.

For the histological preparation, Bone sections containing defect sites were washed thoroughly with normal saline and xed in 10% formalin for 7 days. Subsequently, the bone sections were decalcied in 5% nitric acid and checked regularly for decalcification. Once the bone pieces became exible, transparent and easily penetrable by pins, they were considered to be completely decalcied. The tissues

were processed in a routine procedure and 4 mm sections were cut and stained with haemotoxylin and eosin.

For the morphometric analysis of newly formed bone, the region of bone repair previously identified in the histopathological observation for each specimen was measured, (Five fields were measured from each specimens). The data were obtained using Leica Qwin 500 image analyzer computer system (England).

For bone mineral density, Dual-energy X-ray absorptiometry (DEXA) machine with the software for small animals present at the National Center for Research, was used for measuring bone mineral density of the regenerated bone.

For bone mineral composition determination, using Scanning Electron Microscope (SEM Model Quanta 250) FEG (Field Emission Gun) attached with EDX Unit (Energy Dispersive X-ray Analyses), with accelerating voltage 30 K.V., magnification 14x up to 1000000 and resolution for Gun.1n) was used in this study.

All The specimens that were used for EDX were at first scanned by (DEXA).

Then all the data were submitted to ANOVA and Tukey's test.

Statistical analysis

Data management and statistical analysis were performed using the Statistical Package for Social Sciences (SPSS) version 18. Numerical data were summarized using means and standard deviations. Data were explored for normality by checking the data distribution and using Kolmogorov-Smirnov and Shapiro-Wilk tests.

Comparisons between the 2 groups with respect to normally distributed numeric variables were done using the independent t-test. Comparison of 2 and 4 weeks within the same group was performed by paired t test.

Pearson correlation test was used to study correlation between clinical and radiographic results. The Pearson correlation coefficient is used to measure the strength of a linear association between two variables, as follows:

Exactly -1 . A perfect negative linear relationship.

0 No linear relationship

Exactly $+1$. A perfect uphill (positive) linear relationship

All p-values are two-sided. P-values ≤ 0.05 were considered significant.

RESULTS

Histological analysis revealed that; on the 2 weeks post-surgery, all animals presented the empty defect holes filled by delicate and intertwined bone trabeculae, and the intertrabecular space filled by conjunctive tissue. The neoformed trabeculae contained large osteocytes and were surrounded by cuboid osteoblasts in all specimens (Fig. 1)



Fig. (1): A Photomicrograph of empty holes (2 weeks postoperatively) showing: empty holes filled with delicate bone trabeculae (*), connective tissue (green arrow), large osteocyte (blue arrow), bone trabeculae surrounded by cuboid osteoblasts (black arrow) (H&E, 200X)

While in nano bone filled bone defect microscopic examination most of the nano bone granules located within the bony defects were surrounded by new trabecular bone tissue. Areas of woven bone

could be detected among the growing bone trabeculae. Haversian canal was detected in neobone trabeculae (Fig. 2).

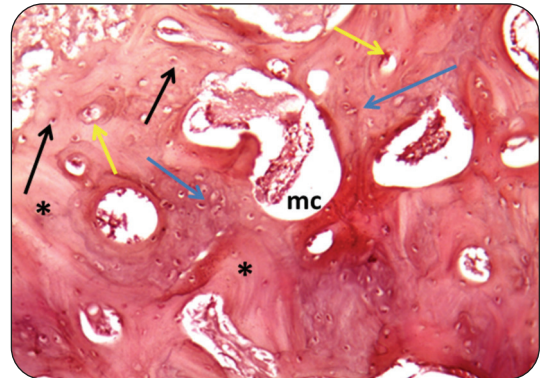


Fig. (2): A Photomicrograph of NanoBone holes (2 weeks postoperatively) showing: newly formed bone trabeculae (blue arrows) enclosing fibrocellular marrow cavities (mc), immature primary bone trabeculae devoid of osteocytes (*), haphazard distributed osteocytes which appeared normal within their lacunae (black arrows), Haversian canal (yellow arrows). (H&E, 200X)

After 4 weeks: More than 90 % of the critical size of empty defect holes has re-grown with new bone trabeculae enclosing variable sized haversian canals (Fig. 3).



Fig. (3): A Photomicrograph of empty holes (4 weeks postoperatively) showing: primary new osteons (*), vascular marrow cavities (black arrow), osteocytes (blue arrow). (H&E, 200X)

In nano bone filled defects, all specimens were characterized by a layer of neoformed bone joining the borders of the defect, as a bridge, The neoformed

bone trabeculae were dense and the intertrabecular fibrous conjunctive tissue was substituted by hematopoietic tissue in all specimens. The bone trabeculae contained small osteocytes, reverse lines, and flattened osteoblasts in the periosteal region. At the surgical borders, there was union of the neoformed bone with the mature adjacent bone (Fig. 4).



Fig. 4): A Photomicrograph of NanoBone holes (2 weeks postoperatively) showing: regularly distributed mature lamellar bone (*), haversian system configuration (black rings), osteocytes (black arrow) (H&E, 200X)

Statistical analysis

I-For Histological results

I-a- Comparison between groups

At 2 weeks, a higher mean value was recorded

in nano group (74.96 ± 11.33), in comparison to 54.67 ± 11.64 in empty group, with a mean difference between groups (26.42 ± 4.02). Independent t test revealed that the difference was statistically significant ($p=0.00$), (Table 1, Fig.5)

At 4 weeks, a higher mean value was recorded in nano group (57.32 ± 10.84), in comparison to 30.90 ± 8.75 in empty group, with a mean difference between groups (20.30 ± 4.69). Independent t test revealed that the difference was statistically significant ($p=0.00$), (Table 1, Fig.5)

I-b- Comparison of 2 and 4 weeks within the same group

In empty group, a higher mean value was recorded at 4 weeks (54.67 ± 11.64), in comparison to 30.90 ± 8.75 at 2 weeks, with a mean difference between both observations was (23.77 ± 4.20). Independent t test revealed that the difference was statistically significant ($p=0.00$), (Table 2, Fig.5)

In nano group, a higher mean value was recorded at 4 weeks (74.96 ± 11.33), in comparison to (57.32 ± 10.84) at 2 weeks, with a mean difference between groups (17.65 ± 4.53). Independent t test revealed that the difference was statistically significant ($p=0.00$), (Table 2, Fig.5)

Table (1) Descriptive statistics and comparison of area percent in both groups (independent t test)

		Mean	Std. Dev.	Difference		95% Confidence Interval of the Difference		T	P
				Mean	Std. Error	Lower	Upper		
2 weeks	Empty	30.90	8.75	-26.42	4.02	-34.78	-18.06	-6.57	.00*
	Nano	57.32	10.84						
4 weeks	Empty	54.67	11.64	-20.30	4.69	-30.02	-10.57	-4.33	.00*
	Nano	74.96	11.33						

Significance level $p \leq 0.05$, *significant

Table (2) Comparison of area percent histological results at 2 and 4 weeks within the same group (paired t test)

		Mean	Std. Dev.	Difference		95% Confidence Interval of the Difference		T	P
				Mean	Std. Error	Lower	Upper		
Empty	2 weeks	30.90	8.75	-23.77	4.20	-32.52	-15.01	-5.66	.00*
	4 weeks	54.67	11.64						
Nano	2 weeks	57.32	10.84	-17.65	4.53	-27.04	-8.25	-3.90	.00*
	4 weeks	74.96	11.33						

Significance level $p \leq 0.05$, *significant

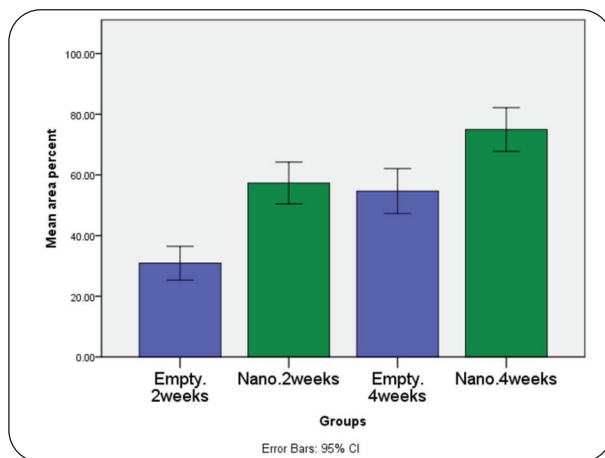


Fig. (5) Bar chart illustrating histological area percent results in both groups at 2 and 4 weeks

II-Results of bone density

II-a- Comparison between groups

At 2 weeks, a higher mean value was recorded in nano group (0.21 ± 0.01), in comparison to 0.17 ± 0.00 in empty group, with a mean difference between groups (0.04 ± 0.00). Independent t test revealed that the difference was statistically significant ($p=0.00$), (Table 3, Fig.6)

At 4 weeks, a higher mean value was recorded in nano group (0.24 ± 0.01), in comparison to 0.18 ± 0.00 in empty group, with a mean difference between groups (0.06 ± 0.00). Independent t test revealed that the difference was statistically significant ($p=0.00$), (Table 3, Fig.6)

II-b- Comparison of 2 and 4 weeks within the same group

In empty group, a higher mean value was recorded at 4 weeks (0.18 ± 0.00), in comparison to 0.17 ± 0.00 at 2 weeks, with a mean difference between both observations was (0.01 ± 0.00). Independent t test revealed that the difference was statistically significant ($p=0.00$), (Table 4, Fig.3)

In nano group, a higher mean value was recorded at 4 weeks (0.24 ± 0.01), in comparison to (0.21 ± 0.01) at 2 weeks, with a mean difference between groups (0.03 ± 0.00). Independent t test revealed that the difference was statistically significant ($p=0.00$), (Table 4, Fig.3)



Table (3) Descriptive statistics and comparison of DEXA in both groups (independent t test)

		Mean	Std. Dev.	Difference		95% Confidence Interval of the Difference		T	P
				Mean	Std. Error	Lower	Upper		
2 weeks	Empty	.17	.00						
	Nano	.21	.01	-.04	.00	-.04	-.03	-18.20	.00*
4 weeks	Empty	.18	.00						
	Nano	.24	.01	-.06	.00	-.06	-.05	-18.32	.00*

Significance level $p \leq 0.05$, *significant

Table (4) Comparison of DEXA results at 2 and 4 weeks within the same group (paired t test)

		Mean	Std. Dev.	Difference		95% Confidence Interval of the Difference		T	P
				Mean	Std. Error	Lower	Upper		
Empty	2 weeks	.17	.00						
	4 weeks	.18	.00	-.01	.00	-.01	-.01	-11.82	.00*
Nano	2 weeks	.21	.01						
	4 weeks	.24	.01	-.03	.00	-.04	-.03	-9.46	.00*

Significance level $p \leq 0.05$, *significant

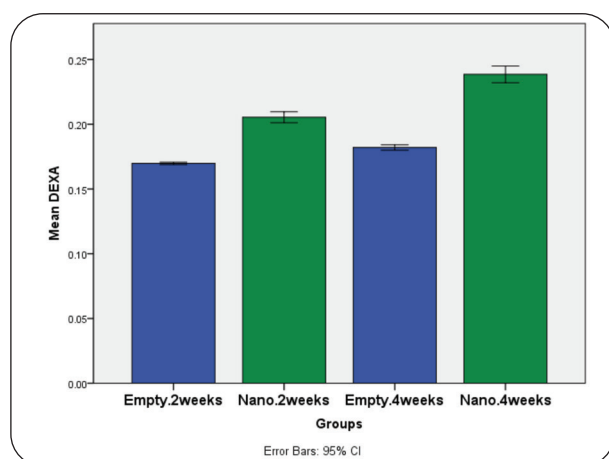


Fig. (6) Bar chart illustrating DEXA results in both groups at 2 and 4 weeks

III-Results of Calcium and Phosphorus value

III-a- Comparison between groups

Calcium

At 2 weeks, a higher mean value was recorded in nano group (21.28 ± 0.02), in comparison to 8.59 ± 0.04 in empty group, with a mean difference between groups (12.7 ± 0.01). Independent t test revealed that the difference was statistically significant ($p=0.00$), (Table 5, Fig.7)

At 4 weeks, a higher mean value was recorded in nano group (32.11 ± 0.04), in comparison to 21.8 ± 0.03 in empty group, with a mean difference between groups (10.31 ± 0.01). Independent t test revealed that the difference was statistically significant ($p=0.00$), (Table 5, Fig.7)

Phosphorus

At 2 weeks, a higher mean value was recorded in nano group (7.16 ± 0.03), in comparison to 2.82 ± 0.07 in empty group, with a mean difference between groups (4.33 ± 0.02). Independent t test revealed that the difference was statistically significant ($p=0.00$), (Table 5, Fig.7)

At 4 weeks, a higher mean value was recorded in nano group (15.84 ± 0.11), in comparison to 10.45 ± 0.03 in empty group, with a mean difference between groups (5.39 ± 0.03). Independent t test revealed that the difference was statistically significant ($p=0.00$), (Table 5, Fig.7)

III-b- Comparison of 2 and 4 weeks within the same group

Empty group

Regarding Calcium, a higher mean value was recorded at 4 weeks (21.8 ± 0.03), in comparison to 8.59 ± 0.04 at 2 weeks, with a mean difference between both observations was (13.21 ± 0.01). Independent t test revealed that the difference was

statistically significant ($p=0.00$), (Table 6, Fig.7)

Regarding Phosphorus, a higher mean value was recorded at 4 weeks (10.45 ± 0.03), in comparison to (2.82 ± 0.07) at 2 weeks, with a mean difference between groups (7.62 ± 0.02). Independent t test revealed that the difference was statistically significant ($p=0.00$), (Table 6, Fig.7)

In nano group

Regarding Calcium, a higher mean value was recorded at 4 weeks (32.11 ± 0.04), in comparison to 21.28 ± 0.02 at 2 weeks, with a mean difference between both observations was (10.83 ± 0.01). Independent t test revealed that the difference was statistically significant ($p=0.00$), (Table 6, Fig.7)

Regarding Phosphorus, a higher mean value was recorded at 4 weeks (15.84 ± 0.11), in comparison to (7.16 ± 0.03) at 2 weeks, with a mean difference between groups (8.68 ± 0.03). Independent t test revealed that the difference was statistically significant ($p=0.00$), (Table 6, Fig.7)

Table (5) Descriptive statistics and comparison of EDX results in both groups (independent t test)

		Mean	Std. Dev.	Difference		95% Confidence Interval of the Difference		T	P	
				Mean	Std. Error	Lower	Upper			
Calcium	2 weeks	Empty	8.59	.04	-12.70	.01	-12.72	-12.67	-964.66	.00*
		Nano	21.28	.02						
	4 weeks	Empty	21.80	.03	-10.31	.01	-10.34	-10.29	-768.26	.00*
		Nano	32.11	.04						
Phosphorus	2 weeks	Empty	2.82	.07	-4.33	.02	-4.38	-4.29	-206.46	.00*
		Nano	7.16	.03						
	4 weeks	Empty	10.45	.03	-5.39	.03	-5.46	-5.32	-165.90	.00*
		Nano	15.84	.11						

Significance level $p \leq 0.05$, *significant



Table (6) Comparison of EDX results at 2 and 4 weeks within the same group (paired t test)

			Mean	Std. Dev.	Difference		95% Confidence Interval of the Difference		T	P
					Mean	Std. Error	Lower	Upper		
Empty	Calcium	2 W	8.59	.04	-13.21	.01	-13.24	-13.18	-933.15	.00*
		4 W	21.80	.03						
	Phosphorus	2 W	2.82	.07	-7.62	.02	-7.67	-7.58		
		4 W	10.45	.03						
Nano	Calcium	2 W	21.28	.02	-10.83	.01	-10.86	-10.81	-875.71	.00*
		4 W	32.11	.04						
	Phosphorus	2 W	7.16	.03	-8.68	.03	-8.75	-8.61		
		4 W	15.84	.11						

Significance level $p \leq 0.05$, *significant

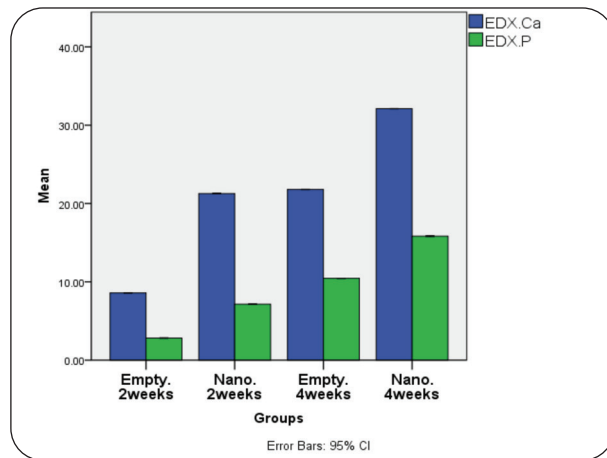


Fig. (7) Bar chart illustrating EDX results in both groups at 2 and 4 weeks

IV- Correlation between Bone density using DEXA and Calcium & Phosphorus value using EDX

DEXA showed a strong positive correlation with EDX calcium and phosphorus ($p=0.00$), (Table 7, Fig. 8-9)

EDX calcium and EDX phosphorus showed a strong positive correlation ($p=0.00$), (Table 7, Fig.10)

Table (7) Correlation between Bone density using DEXA and Calcium & Phosphorus value using EDX results (Pearson correlation test)

		DEXA	EDX.Ca	EDX.P
DEXA	Pearson Correlation (R)	====	.881**	.811**
	P		.000	.000
	Significance		Strong positive	Strong positive
EDX.Ca	Pearson Correlation (R)	.881**	====	.967**
	P	.000		.000
	Significance	Strong positive		Strong positive
EDX.P	Pearson Correlation (R)	.811**	.967**	====
	P	.000	.000	
	Significance	Strong positive	Strong positive	

Significance level $p \leq 0.05$, *significant

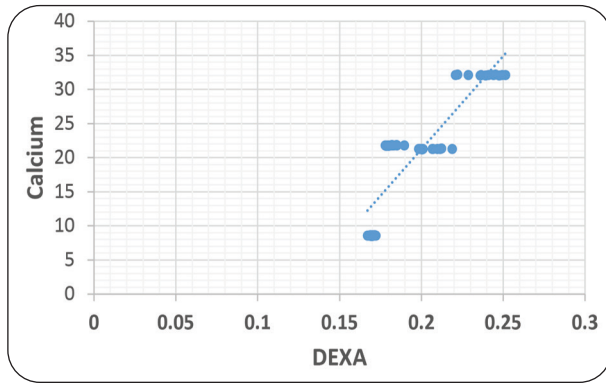


Fig. (8) Scatter plot showing correlation between DEXA and EDX calcium results

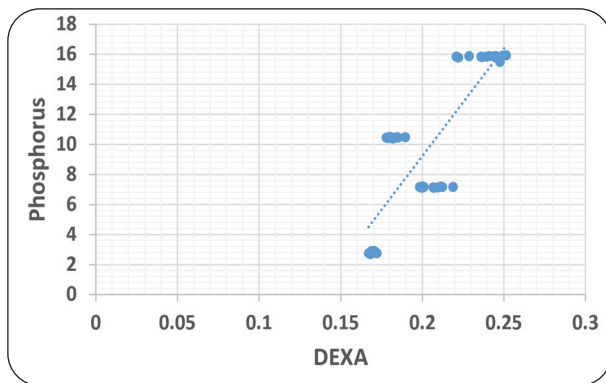


Fig. (9) Scatter plot showing correlation between DEXA and EDX phosphorus results

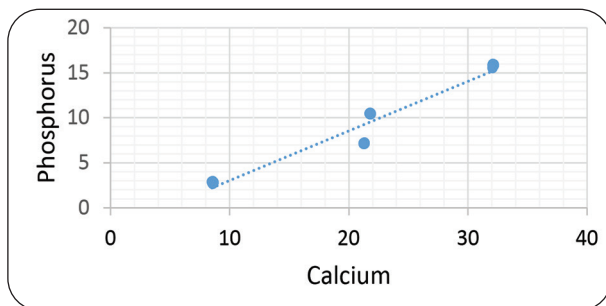


Fig. (10) Scatter plot showing correlation between EDX calcium and phosphorus results

DISCUSSION

Although autogenous bone grafts are considered the gold standard for bone regeneration, they have certain limitations, including patient morbidity at the harvest site. Synthetic bone substitutes have been developed to overcome some of these limitations.

Thus, the aim of this study is to correlate between DEXA and EDX after bone healing in an animal model after using bone substitutes.

The rabbit was chosen in this study due to ease of handling and observing as it's very docile and non-aggressive, On other hand their bones heal faster, only 6 weeks was needed for osseointegration to take place. In addition to some similarities are reported in the bone mineral density and subsequently the fracture toughness of mid-diaphyseal bone between rabbits and human beings ⁽²⁶⁾.

The tibia was chosen instead of jaw, as it provides a beneficial surgical site, since it is not affected by bacterial infection and trauma from chewing, also the double layer suturing (first deep soft tissue and then the skin) prevents unwanted wound site exposure.

The diameter of the defect greatly influences the rate, speed, and quality of healing ⁽²⁷⁾. In animal models, defects greater than 3 mm in diameter tend to heal slower than smaller defects. In current study we made standardized defects of 3 mm diameters ⁽²⁸⁾

It is essential to verify whether the substituted material complied with the concept of "critical size defects". This concept has different thresholds according to the animal species and the site of the defect.

Almeida J, 2007; Arisawa E, 2008; Nascimento S, 2010 considered that, surgical circumscribed bone defects in the rat femur with a recommended standard 3.7 mm diameter, is the critical hole size ⁽²⁹⁻³¹⁾.

DEXA was used to measure bone density. DEXA is useful for verifying the effects of food or medicines on bone disease such as osteoporosis by analysis BMD changes. Other benefits include cost effectiveness and less time consuming. ^(32,33)

Energy-dispersive x ray (EDX) microanalysis involves analysis of x rays with energies characteristic of the atoms in the specimen emitted when an incident electron hits the specimen surface. Analysis



of these x rays can provide elemental maps of the distribution of important elements such as Ca, P, F, and Sr within the specimen. EDX analysis provides accurate information on the chemical elements present in the biomaterial and surrounding tissues, discloses the graft's resorptive changes, and may reveal changes in healing process⁽³⁴⁾. The elemental analysis of the current study was done using EDX for calcium (Ca) and phosphorus (P) which are the main constituents of hydroxyapatite crystals that represent the main component of the inorganic part of the bone tissue⁽³⁵⁾.

However, EDX techniques had some limitations, it does not provide an in vivo description of the tissues surrounding the graft material, neither quantifying the percentage of new bone, residual graft nor connective tissue. Also the need to dehydrate and coat the specimen with a conductive coating^(36,37). Thus, complementary histological analysis was done.

The histological results in the present investigation showed different histological pattern of bone regeneration between all experimental groups. In group I (2 weeks postoperatively) the empty holes revealed delicate irregularly very thin newly formed bone trabeculae. On other hand the neoformed bone in other experimental treated holes appear more thicker than that of empty. The newly formed bone trabeculae was immature and lacked Haversian pattern. These trabeculae enclosed fibrocellular marrow cavities as well as enclosing randomly distributed osteocytes in some areas and devoid of osteocytes in other areas.

The presence of granulation tissue is considered an evidence of early stages of healing. **Marquez et al., 2013** described the healing process of the tooth sockets as it follows a well-defined course, showing typical histological features of the bone healing stages including inflammation, formation of granulation tissue and primary bone tissue as well as its replacement by lamellar bone.⁽³⁸⁾

In group II (4 weeks postoperatively) of the current study the histological analysis showed advance in the course of bone healing in the experimental groups. In empty holes the newly formed bone exhibited primary new osteons and enclosed variable size of marrow cavities. The neoformed bone displayed small island of woven bone as well as randomly distributed osteocytes. On other hand, the NanoBone treated holes showed multiple primary osteon taking Haversian system conformation. The bone lamellae become more organized enclosed normally appeared osteocytes within their lacunae.

Such results in 4 and 6 weeks were in accordance with the histomorphometric results which revealed that a higher mean value was recorded in nano group, in comparison to empty group. The difference between groups was statistically significant.

The results of histology consistence with (Lin K, et al., 2014, Dau M, et al., 2016, Abdel Hamid, D et al., 2018) who monitored the behaviour of Nano Bone by means of histologic and histomorphometric analyses.^(39,40,41)

The noninvasive (DEXA) and invasive (EDX) methods in BMD measurements of small animals were carried out to complement the information already obtained from histological analysis.

In the present study DEXA was used for the elemental analysis for calcium and phosphorous and to compare their different percentages in the newly formed bone. This in accordance with Mossaad Aida M et al 2021 who used DEXA as a rapid diagnostic tool to determine the densitometric quality of regenerated bone at the site of bone marrow and platelet-rich membrane grafting technique at unilateral alveolar cleft region.⁽⁴²⁾

In the present study the bone density measurement at all evaluation periods showed the lowest value was recorded in empty holes and the highest value was recorded in nano groups. This means that the bone density was increased with NanoBone groups.

EDX microanalysis confirmed the expected changes in mineral contents and correlated with the bone density measurement

EDX measurement revealed that the higher mean value of both calcium and phosphorus was recorded in nano groups, in comparison to empty groups. The difference between groups was statistically significant.

Our results were in accordance with Nitin S, et al., 2016 who studied the ability of a functionally designed 3D scaffold to bridge critical size defects and induce new bone formation in a New Zealand white rabbit tibial model, and evaluated the Ca and P content using a combination of techniques from week 2 to 25. One of them was energy dispersive X-ray (EDX). EDX analysis showed the Ca/P value to be 1.63 for the normal bone. It was shown that a deviation from the ideal hydroxyapatite stoichiometry value of Ca/P (1.67) happens in the preliminary stage of bone formation. Such a deviation can be explained on the basis of the presence of a precursor of hydroxyapatite in immature bones. EDX analysis was performed for samples and Ca/P values were found to be nearly 1.67 at 14 and 25 weeks, which was significantly higher than the previous time points, suggesting increased mineral deposition at week 14. They concluded that, A direct correlation was observed between the mineral density in healed bone with time. ⁽⁴³⁾

In regard to correlation between DEXA and EDX: DEXA showed a strong positive correlation with EDX calcium and phosphorus content. On other hand EDX for calcium and phosphorus showed a strong positive correlation to each other. Moreover, a remarkable correlation was observed in the various bone healing parameters used herein, i.e., DEXA, EDX and histology analysis.

Up to our knowledge, This is the first study combining the histology with DEXA and EDX to analyze all elements of bone components.

CONCLUSION

DEXA is a reliable technique to estimate BMD in a non-invasive way, hence allowing for longitudinal studies over longer periods of time while avoiding sacrificing of animals.

DEXA, EDX and histological analysis provide complete insight of bone before and after graft placement which help in assessment bone healing with and without bone graft placement.

The BMC percentage measured by DEXA was significantly correlated with minerals percentage measured by EDX.

DEXA and EDX were in a line with the histological assessment throughout the study.

REFERENCES

1. Mouriño V, Boccaccini AR. Bone tissue engineering therapeutics: controlled drug delivery in three-dimensional scaffolds. *J R Soc Interface* 2010; 7: 209–227.
2. Habibovic P, de Groot K. Osteoinductive biomaterial properties and relevance in bone repair. *J Tissue Eng Regen Med* 2007;1(1):25e32.
3. Traianedes K, Russell JL, Edwards JT, Stubbs HA, Shanahan IR, Knaack D. Donor age and gender effects on osteoinductivity of demineralised bone matrix. *J Biomed Mater Res B Appl Biomater* 2004;70(1):21e9.
4. Habibovic P, Yuan H, van den Doel M, Sees TM, van Blitterswijk CA, de Groot K. Relevance of osteoinductive biomaterials in critical-sized orthotopic defect. *J Orthop Res* 2006; 24(5):867e76.
5. Yao J, Li X, Bao C, Zhang C, Chen Z, Fan H, et al. Ectopic bone formation in adipose-derived stromal cell-seeded osteoinductive calcium phosphate scaffolds. *J Biomater Appl* 2010; 24(7):607e24.
6. Chitsazi MT, Shirmohammadi A, Faramarzie M, Pourabbas R, An Rostamzadeh. A clinical comparison of nano-crystalline hydroxyapatite (ostim) and autogenous bone graft in the treatment of periodontal intrabony defects. *Med Oral Patol Oral Cir Bucal* 2011;16(3):e448e53.
7. Gholami GA, Najafi B, Mashhadiabbas F, Goetz W, Najafi S. Clinical, histological and histomorphometric evaluation of socket preservation using a synthetic nanocrystalline



- hydroxy-apatite in comparison with a bovine xenograft: a randomized clinical trial. *Clin Oral Implants Res* 2012; 23(10):1198e204.
8. Gerike W, Bienengr€aber V, Henkel KO, Bayerlein T, Proff P, Gedrange T, et al. The manufacture of synthetic non-sintered degradable bone grafting substitutes. *Folia Morphol (Warsz)* 2006; 65(1):54e5.
 9. G€otz W, Gerber T, Michel B, Lossd€orfer S, Henkel KO, Heinmann F. Immunohistochemical characterization of nano-crystalline hydroxyapatite silica gel (NanoBone®) osteogenesis: a study on biopsies from human jaws. *Clin Oral Implants Res* 2008; 19(10):1016e26.
 10. Ghanaati S, Udeabor SE, Barbeck M, Willershausen I, Kuenzel O, Sader RA, et al. Implantation of silicone dioxide-based nanocrystalline hydroxyapatite and pure phase beta-tricalciumphosphate bone substitute granules in caprine muscle tissue does not induce new bone formation. *Head Face Med* 2013; 9:1.
 11. G€otz W, Lenz S, Reichert C, Henkel KO, Bienengr€aber V, Pernicka L, et al. A preliminary study in osteoinduction by anano-crystalline hydroxyapatite in the mini pig. *Folia Histo-chem Cytobiol* 2010; 48(4):589e96.
 12. Henkel KO, Gerber T, Lenz S, Gundlach KK, Bienengr€aber V. Macroscopical, histological and morphometric studies of porous bone-replacement materials in minipigs 8 months after implantation. *Oral Surg Oral Med Oral Pathol Oral Radiol Endod* 2006 Nov; 102(5):606e13.
 13. Glimcher MJ, Bonar LC, Grynblas MD, Landis WJ, Roufosse AH. Recent studies of bone mineral: Is the amorphous calcium phosphate theory valid? *J Cryst Growth* 1981; 53: 10G-19.
 14. Peacock, M.: Calcium metabolism in health and disease. *Clin. J. Am. Soc. Nephrol.* 2010; 5: S23–S30
 15. Shapiro, R., Heaney, R.P.: Co-dependence of calcium and phosphorus for growth and bone development under conditions of varying deficiency. *Bone.* 2003; 32: 532–540
 16. Coats, A.M., Zioupos, P., Aspden, R.M.: Material properties of subchondral bone from patients with osteoporosis or osteoarthritis by microindentation testing and electron probe microanalysis. *Calcif. Tissue Int.* 2003; 73: 66–71
 17. Howell PG, Boyde A. Volumes from which calcium and phosphorus X-rays arise in electron probe emission microanalysis of bone: Monte Carlo simulation. *Calcif Tissue Int.* 2003; 72: 745–749.
 18. Lambert JB, Simpson SV, Buikstra JE, Hanson D. Electron microprobe analysis of elemental distribution in excavated human femurs. *Am J Phys Anthropol.* 1983; 62:409–423.
 19. Roschger P, Manjubala I, Zoeger N, Meirer F, Simon R, Li C, Fratzi-Zelman N, Misof B, Paschalis E, Strelci C, Fratzi P, Klaushofer K. Bone material quality in transiliac bone biopsies of postmenopausal osteoporotic women after 3 years of strontium ranelate treatment. *J Bone Miner Res.* 2010; 25:891–900.
 20. Smolders J M, Hol A, Rijnders T, van Susante J L. Changes in bone mineral density in the proximal femur after hip resurfacing and uncemented total hip replacement: a prospective randomised controlled study. *Clin Orthop Relat Res. [Randomized Controlled Trial]* 2010; 92(11): 1509-14.
 21. Lazarinis S, Milbrink J, Mattsson P, Mallmin H, Hailer N P. Bone loss around a stable, partly threaded hydroxyapatite-coated cup: a prospective cohort study using RSA and DXA. *Hip Int* 2014; 24(2): 155-66.
 22. Davey M J M Gerhardt, Enrico De Visser, Baudewijn W Hendrickx, Berend W Schreurs & Job L C Van Susante (2018): Bone mineral density changes in the graft after acetabular impaction bone grafting in primary and revision hip surgery, *Acta Orthopaedica*, 2018; 89(3): 1745-3674.
 23. Recent advances in nano scaffolds for bone repair Huan Yi1 , Fawad Ur Rehman1 , Chunqiu Zhao1 , Bin Liu2 and Nongyue He1,3 *Bone Research* (2016) 4, 16050; doi:10.1038/boneres.2016.50
 24. John O. Akindoyo Suriati Ghazali* Mohammad D. H. Beg Nitthiyah Jeyaratnam. Characterization and Elemental Quantification of Natural Hydroxyapatite Produced from Cow Bone. *Chem. Eng. Technol.* 2019, 42, No. 9, 1805–1815.
 25. Carlo Prati 1,* , Fausto Zamparini 1,2 , Daniele Botticelli 3 , Mauro Ferri 4 , Daichi Yonezawa 5 , Adriano Piattelli 6 and Maria Giovanna Gandolf. The Use of ESEM-EDX as an Innovative Tool to Analyze the Mineral Structure of Peri-Implant Human Bone. *Materials* 2020, 13, 1671.
 26. Manjeet Mapara et al. Rabbit as an animal model for experimental research. *Dent Res J (Isfahan).* 2012 Jan-Mar; 9(1): 111-118
 27. Wang J. Spatial orientation of the microscopic elements of cortical repair bone. *Clin Orthop.* 2000; (374):265-77.
 28. Johan C, Marta M, Hans J, Anne M, Jan E, Staale. Porous titanium granules promote bone healing and growth in rabbit tibia peri-implant osseous defects. *Clin Oral Implants Res.* 2010; 21: 165-73
 29. Almeida, J.D., E.A.L. Arisawa, R.F. da Rocha and Y.R. Carvalhon. Effect of calcitonin on bone regeneration in male rats: a histomorphometric analysis, *International*

- Journal of Oral and Maxillofacial Surgery. 2007; a36(5): 435-440.
30. Arisawa, E.A.L., A.A.H. Brandão, J.D. Almeida and R.F. da Rocha. Calcitonin in bone-guided regeneration of mandibles in ovariectomized rats: densitometric, histologic and histomorphometric analysis, *International Journal of Oral and Maxillofacial Surgery*. 2008; 37(1): 47-53.
 31. Nascimento S.B, Cardoso T.P., Ribeiro. Effect of low-level laser therapy and calcitonin on bone repair in castrated rats: a densitometric study. *Photomedicine and Laser Surgery*. 2010; 28(1): 45-49.
 32. Ho Sung Kim a, Eun Sun Jeong b, Myung Hwa Yang c, Seoung-Oh Yang d. Bone mineral density assessment for research purpose using dual energy X-ray absorptiometry Osteoporosis and Sarcopenia. 2018; 79e85
 33. Maria Permyu1, Monica Lopez-Pena1, Fernando Munoz1, Antonio Gonzalez-Cantalapiedra1. Rabbit as model for osteoporosis research. *Journal of Bone and Mineral Metabolism*. 2019; 37:573–583
 34. Roschger P, Manjubala I, Zoeger N, Meirer F, Simon R, Li C, Fratzl-Zelman N, Misof B, Paschalis E, Strelj C, Fratzl P, Klaushofer K. Bone material quality in transiliac bone biopsies of postmenopausal osteoporotic women after 3 years of strontium ranelate treatment. *J Bone Miner Res*. 2010; 25:891–900.
 35. Avery JK, Chiego DJ. *Essentials of oral histology and embryology: a clinical approach*. 3rd ed. Salt Lake City: Mosby Elsevier; 2006.
 36. Lindgren, C., Hallman, M., Sennerby, L., Sammons, R. Back-scattered electron imaging and elemental analysis of retrieved bone tissue following sinus augmentation with deproteinized bovine bone or biphasic calcium phosphate. *Clin. Oral Implants Res*. 2010; 21: 924–930.
 37. Ramírez-Fernández, M.P., Calvo-Guirado, J.L., Maté-Sánchez del Val, J.E., Delgado- Ruiz, R.A., Negri, B., Barona-Dorado, C., 2012. Ultrastructural study by back-scattered electron imaging and elemental microanalysis of bone-to- biomaterial interface and mineral degradation of porcine xenografts used in maxillary sinus floor elevation. *Clin. Oral Implants Res*. 2012; 00: 1–8.
 38. Marquez L, Fernando A, Cynthia L, Guilherme D, Melissa N, Jose Bento A. Enhanced bone healing of rat tooth sockets after administration of epidermal growth factor (EGF) carried by liposome *Injury, Int. J. Care Injured*. 2013; 44: 558–564.
 39. Lin K, Wu C, Chang J. Advances in synthesis of calcium phosphate crystals with controlled size and shape. *Acta Biomater* 2014; 10:4071–102.
 40. Dau M, Kämmerer PW, Henkel K-O, Gerber T, Frerich B, Gundlach KKH. Bone formation in mono cortical mandibular critical size defects after augmentation with two synthetic nanostructured and one xenogenous hydroxyapatite bone substitute - in vivo animal study. *Clin Oral Implants Res* .2016; 27:597–603.
 41. Abdel Hamid, D, Safa F. Abdel El-Ghanib, Mohamed M. Khashabac. Characterization of nano-hydroxyapatite silica gel and evaluation of its T combined effect with Solcoseryl paste on bone formation: An experimental study in New Zealand rabbits. *Future Dental J*. 2018; 4: 179-287.
 42. Mossaad, Aida M, Ahmady, Hatem H, Ghanem, Wael H, Abdelrahman, Moustapha A, Abdelazim, Ahmed F, Elsayed, Shadia A. The Use of Dual Energy X-Ray Bone Density Scan in Assessment of Alveolar Cleft Grafting Using Bone Marrow Stem Cells Concentrate/Platelet-Rich Fibrin Regenerative Technique. *Journal of Craniofacial Surgery*: 2021; Volume 32 - Issue 8 - e780-e783
 43. Nitin Sagar, Atul Kumar Singh, Mayur K. Temgire, S. Vijayalakshmi, b Alok Dhawan, d Ashutosh Kumar, a Naibedya Chattopadhyay and Jayesh R. Bellare. 3D scaffold induces efficient bone repair: in vivo studies of ultra-structural architecture at the interface *RSC Adv*. 2016; 6, 93768–93776





الأزهر مجلة أسبوت طب الأسنان

النشر الرسمي لكلية طب الأسنان
جامعة الأزهر أسيوط
مصر

AADJ, Vol. 5, No. 2, October (2022) — PP. 191

رابطة DEXA مع EDX في تقييم مكونات العظام غير العضوية بعد تطبيق عظم النانو لإصلاح عيب العظام

نجلاء الكيلاني¹, نهاد احمد²*

1. قسم طب الفم وأمراض اللثة، والتشخيص والأشعة، كلية طب الأسنان، جامعة الأزهر، أسيوط، مصر
 2. قسم بيولوجيا الفم والأسنان، كلية طب الأسنان، جامعة الأزهر، القاهرة، بنات، مصر
- * البريد الإلكتروني NEHADMUHAMMED.26@AZHAR.EDU.EG

الملخص :

الهدف: الهدف من هذه الدراسة هو ربط داكسا وادكس في تقييم الاختلافات في التركيب الكيميائي من حيث العناصر الرئيسية التي تتكون من معدن العظام الكالسيوم (CA) والفوسفور (P) بعد تطبيق عظم النانو لإصلاح عيب العظام.

المواد والاساليب: تم إنشاء عيب حفر العظام في الساق اليمنى (فتحتان في كل قصبه) لـ 48 أرنبًا. وترك الفتحة العلوية فارغة بينما كانت الحفرة السفلية مليئة بعظم النانو. تم التضحية بـ 24 حيوانًا بعد أسبوعين من الجراحة. وتم التضحية بالحيوانات المتبقية بعد 4 أسابيع. تم تحضير نصف العينات العظمية للمعالجة الجبرية الروتينية والنسجية والقياسات النسيجية، بينما تم مسح العينات المتبقية بواسطة قياس امتصاص الأشعة السينية ثنائي الطاقة (داكسا) لقياس كثافة المعادن في العظام ثم تم استخدامها لتحديد تكوين المعادن في العظام بواسطة الطاقة المشتتة لخلايا الأشعة السينية (ادكس) تمت مقارنة قياسات DEXA و EDX بعد ذلك. تم تقديم البيانات إلى اختبار انوفا وتوكي.

النتائج: أن داكسا أظهر علاقة إيجابية قوية مع ادكس والتحليل النسيجي.

الخلاصة: يعد التحليل المجهرى للأشعة السينية المشتتة للطاقة أداة كمية مفيدة لتحليل الكالسيوم والفوسفور في العظام بطريقة غير جراحية.

الكلمات المفتاحية: عظم النانو، داكسا، ادكس، الأرناب، معادن العظم